Supplementary Information for:

Photogenerated charge carriers dynamics on Pt loaded SrTiO$_3$ nanoparticles studied by transient-absorption spectroscopy

Fumihiko Ichihara [a,b], Hong Pang* [a,b], Tetsuya Kako [a], Detlef W. Bahnemann [c], Jinhua Ye* [a,b]

a Research Center for Materials Nanoarchitectonics (MANA), National Institute for Materials Science

(NIMS), 1-1 Namiki, Tsukuba, Ibaraki 305-0044, Japan.

b Graduate School of Chemical Sciences and Engineering, Hokkaido University, Sapporo 060-0814,

Japan.

c Institute for Technical Chemistry, Leibniz University Hannover, Hannover 30167, Germany.

Corresponding author:
PANG.Hong@nims.go.jp; Jinhua.YE@nims.go.jp

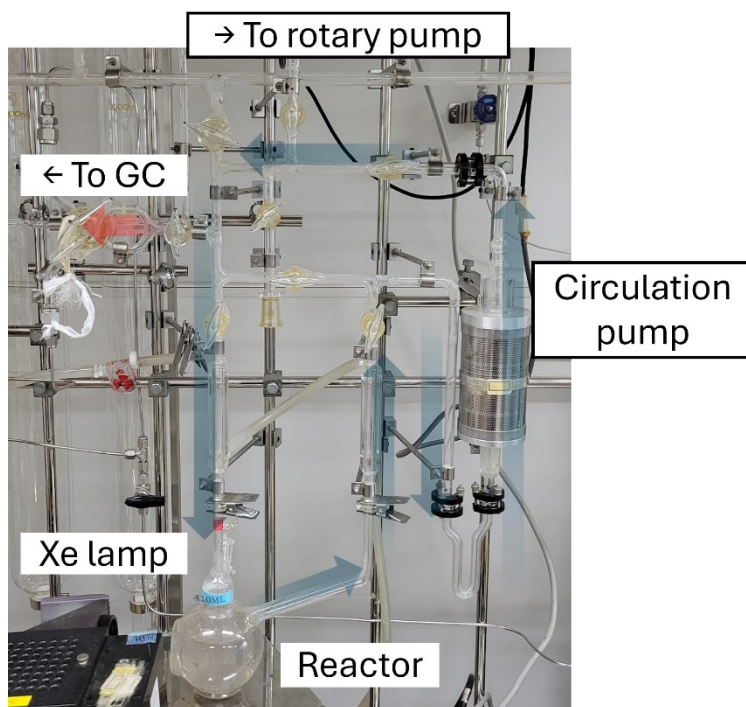## 1. Photocatalytic activity evaluation system

Figure S1. The picture of photocatalytic activity evaluation system

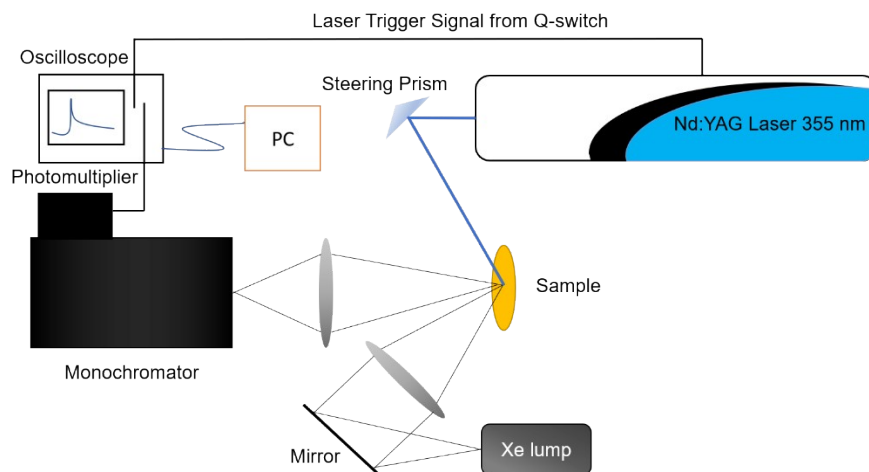## 2.Nano-micro second transient absorption spectroscopy

Figure S2. Schematic diagram of the set-up for nano-micro second transient absorption spectroscopy

In this set-up[1], a Q-switched Nd:YAG laser (Quantel; Brilliant B, third harmonics, 355 nm, 10 Hz) served as the excitation light, with a pulse duration of 20 ns. Following the photo-excitation of sample, a 150 W Xe lamp was used as the probe light source to analyze the absorption of transient species. The

probe light was focused onto the surface of solid samples by using optical lens. The diffusely reflected probe light was then collected by another different optical lens and directed to a monochromator by a plane-folding mirror. The dispersed light from the monochromator was captured by a photomultiplier detector (Hamamatsu R928), which converted the optical signals to electric signals. These signals were subjected into a distal oscilloscope via tunable signal terminator. The oscilloscope recorded the data points as voltage changes, which could then be converted to transient absorption, ΔJ, using the following equation: (eq. 1)

$$\Delta J = \frac{J_0/I_0 - J_x/I_0}{J_0/I_0} = \frac{J_0 - J_x}{J_0} \quad (1)$$

where I_0 is the intensity of probe light, J_0 is the signal intensity of diffusely reflected probe light without excitation, and J_x is the signal of diffusely reflected probe light when irradiated by the excitation laser pulse.

The recorded decay signal ΔJ was fitted to a fractal fit function[2] (eq. 2)

$$\Delta J = \frac{A(1-h)}{(1-h) + Ak_{2,f}t^{1-h}} \quad (2)$$

, where A represents the intensity of the transient signals, and the exponent h denotes the fractal dimension of the surface, and the decay constant $k_{2,f}$ is associated with the trapping and recombination of charge carriers.

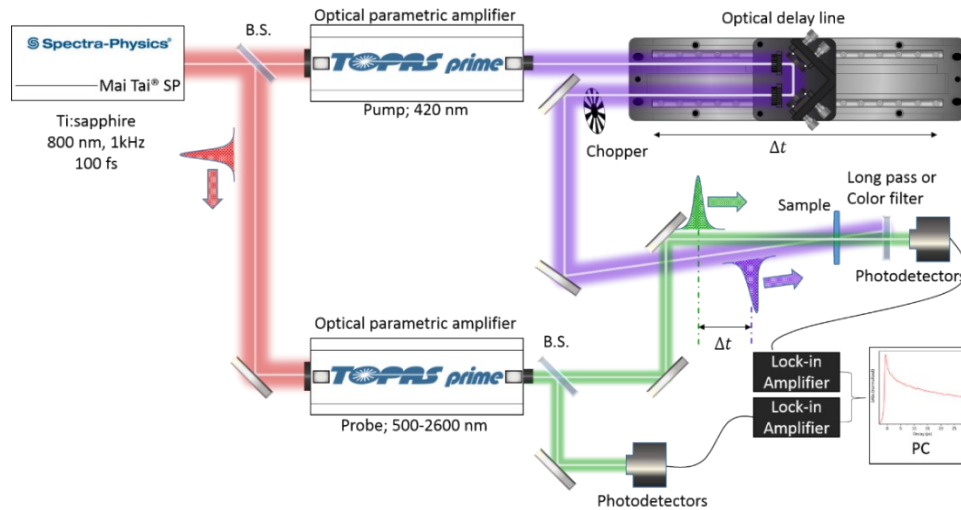## 3. Pico-nano second transient absorption spectroscopy

Figure S3. Schematic diagram of the set-up for the pico-nano second transient absorption spectroscopy

In an ultrafast transient absorption setup[3], the light source of 1 kHz Ti:sapphire regenerative amplifier (Solstice, Spectra-Physics) generates pulses with ~100 fs duration and a wavelength of 800 nm with a bandwidth of ~20 nm. To perform transient absorption spectroscopy with the Ti:sapphire laser alone, the laser beam is split into two parts. One beam is restricted to a wavelength region for the excitation pulse around 800 nm while the other is further split into two beams. In order to shift the wavelength to other regions of the visible and near-IR spectra, optical parametric amplifiers (OPAs) are typically employed. In an OPA, non-linear birefringent crystals, such as beta barium borate (BBO), are pumped by the direct output of the amplified laser system at 800 nm or by frequency-doubled pulses at 400 nm. The pumps are temporally and spatially overlapped in the crystal, and depending on the angle between the laser beam and the crystal's symmetry axis, two particular wavelengths of the white-light continuum, called "signal" and "idler", are amplified through the second-order nonlinear polarizability of the crystal. In this crystal, the signal has the shortest wavelength and is routinely selected for further use. Since the signal and idler beams have different polarizations, their group velocity, signal, and idler beams can be made equal by adjusting the angle between the laser beam and the symmetry axis of the birefringent crystal in the OPA (TOPAS prime, Light Conversion Ltd.). This adjustment allows energy from the light source beam to be efficiently converted to the signal and idler beams over a large conversion length, up to the order of millimeters. This is known as phase-matching condition. In this case, by modifying the phase-matching condition, the signal frequency and idler frequency can be tuned to maintain the light energy. Thus, when 800 nm light source was applied as pump, the OPA can generate a near-infrared (IR) signal in the range of 1,100–2,600 nm while the visible spectrum in the range of 475–750 nm can be generated by a 400 nm pump. By using the output of an OPA as the fundamental, all wavelengths from the Ultra-Violet (UV) to mid-IR can be generated at relatively high pulse energies by applying non-linear mixing processes such as frequency-doubling and sum-frequency generation in suitable non-linear crystals. UV to mid-IR light are the most useful wavelengths for the study of photocatalytic systems.

To initiate the time delay between the excitation and probe pulses, the excitation pulse generated by OPA passes through an optical delay line, which consists of two mirrors mounted on a punctual motorized computer-controlled moveable stage. The optical delay line employed in our experiments has an accuracy and reproducibility of 0.1 μm, corresponding to a timing accuracy of 0.5 fs. The delay

line is able to move over a maximum range of 200 mm, allowing for the time delays up to 1.25 ns between pump and probe beams.

At last, both excitation light and probe lights were focused and overlapped on the surface of the photocatalysts. The transmitted probe light was focused onto Si or InGaAs photodetectors, with detection ranges of 500-1000 and 1000-2600 nm. Scattered excitation light was blocked by a long-wave pass filter placed in front of the photodetectors. The intensity of the transmitted probe light, T, was detected by amplifying the signal from the probe light using a lock-in amplifier synchronized with the 1 kHz repetition rate of the probe light pulsed. The change in the intensity of the transmitted probe light caused by the excitation light $\Delta T(t)$, was detected by the differential amplification of the signal from probe light and that from the reference light using a lock-in amplifier synchronized with the frequency of the optical chopper, where t is the time delay between pump and probe pulses generated by optical delay line.

For the measurement of transient absorption spectra, the wavelength of the probe light was measured over the range from 500 to 2600 nm, while the measurement for the signal decay for the transient absorption was performed by scanning the delay time, up to a maximum of approximately 1 ns, using the optical delay line.
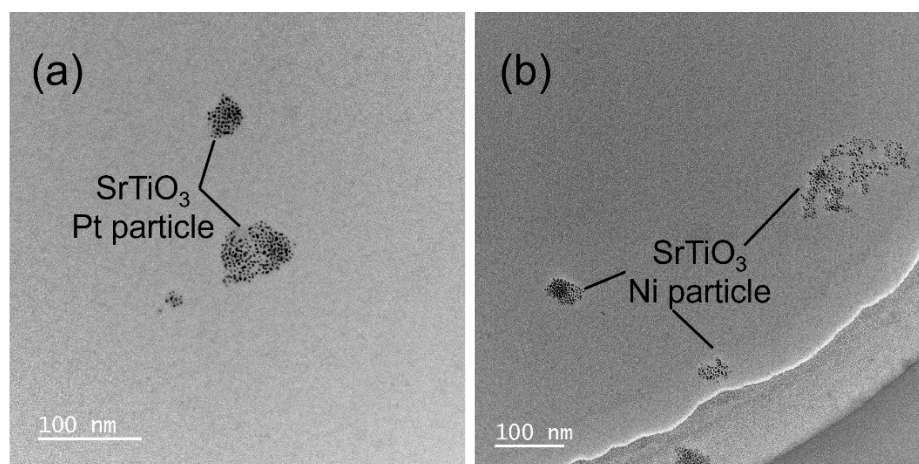
4. TEM observations

Figure S4. TEM image of (a) Pt and (b) Ni 1.0wt% loaded SrTiO₃

Figure S4 shows TEM image of (a) Pt and (b) Ni 1.0wt% loaded $SrTiO_3$, the Pt and Ni cocatalysts were well dispersed on $SrTiO_3$ and the diameter of Pt nanoparticle was about 4 nm, while the diameter of Ni nanoparticle was about 2 nm. The actual loading amount of the cocatalyst was estimated to be

0.94wt% for Pt and 0.95wt% for Ni, assuming that Pt and Ni were loaded as metallic states, which is relatively consistent with the 1.0wt% loading amount of the cocatalyst preparation value.
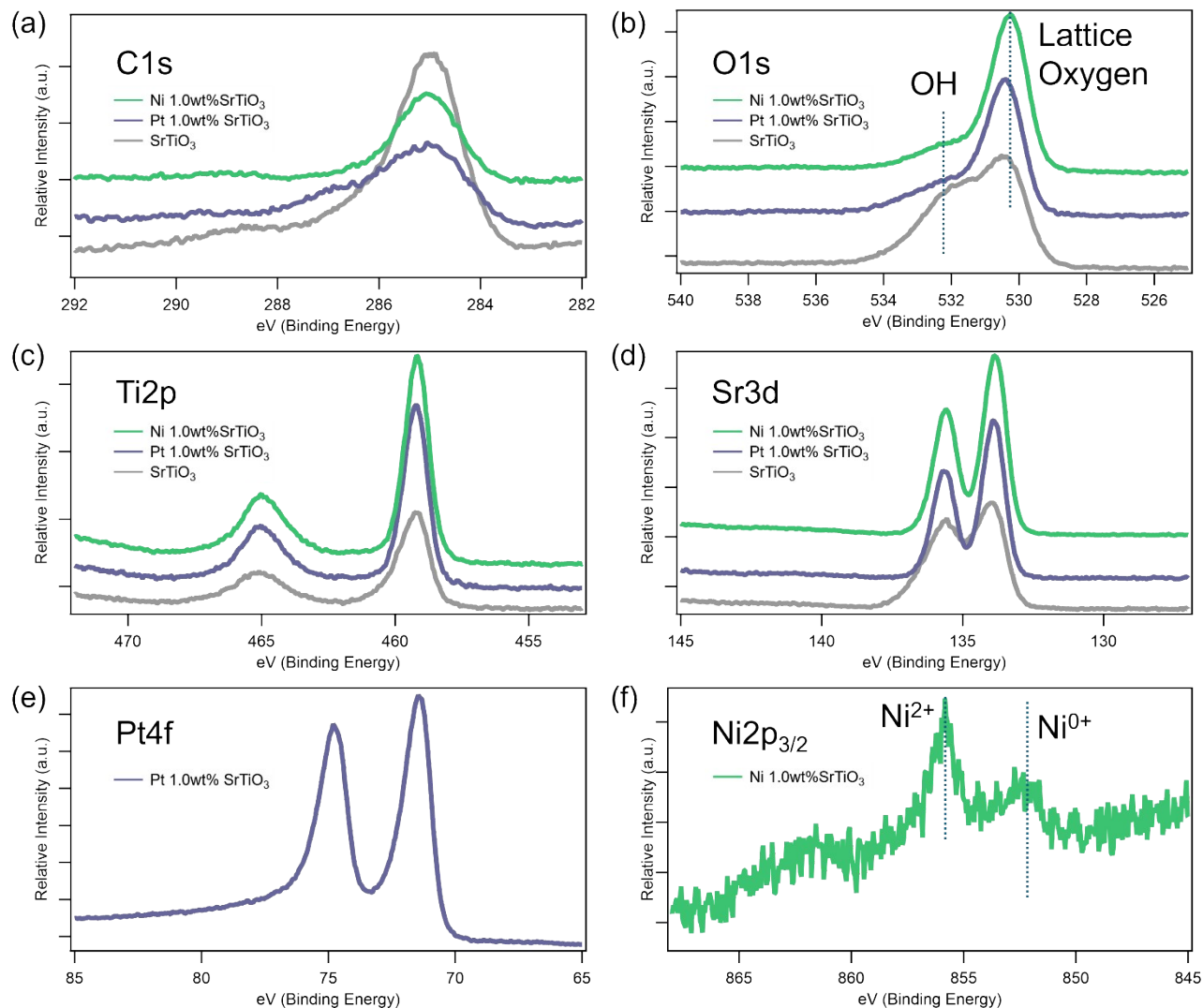
5. XPS measurements

Figure S5. XPS spectra of (a) C1s, (b) O1s, (c) Ti2p, (d) Sr3d, (e) Pt4f and (f) Ni2p$_{3/2}$ of Pt and Ni 1.0wt% loaded SrTiO$_3$.
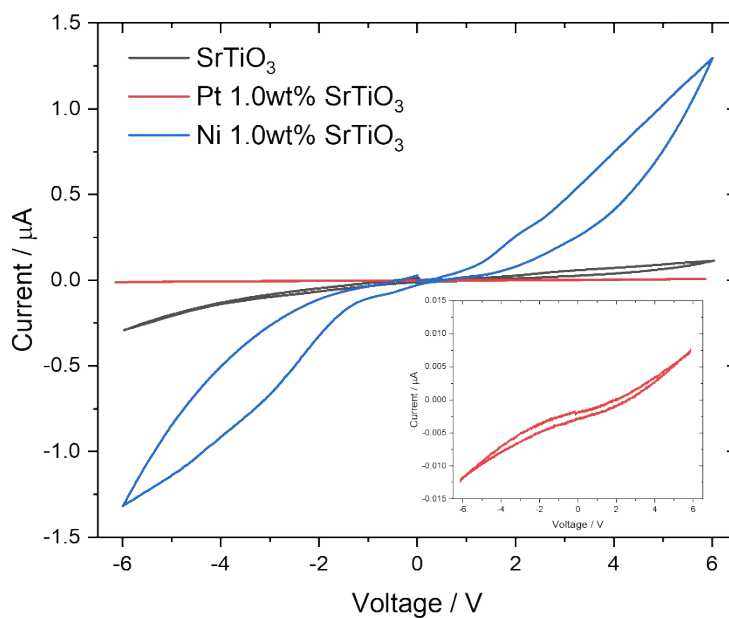
6. I-V curve measurements

Figure S6. I-V curves of Pt and Ni 1.0wt% loaded SrTiO₃
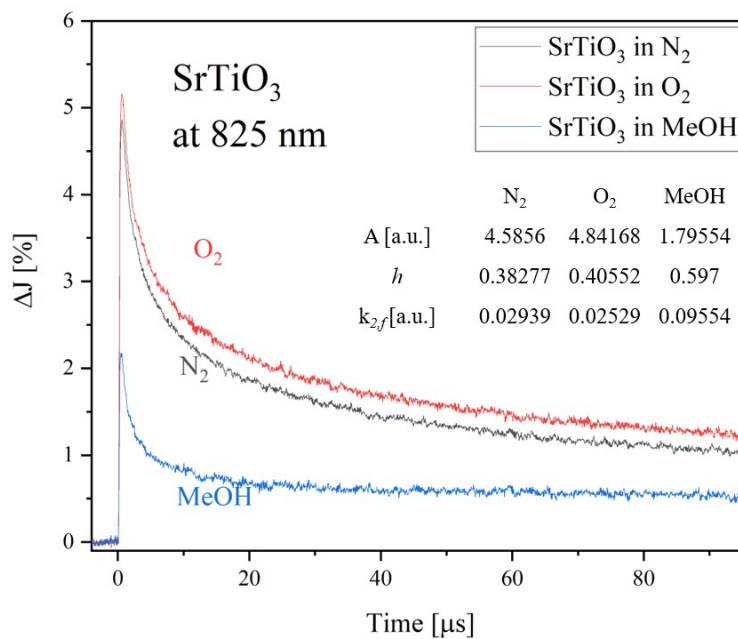
7. Transient absorption measurements

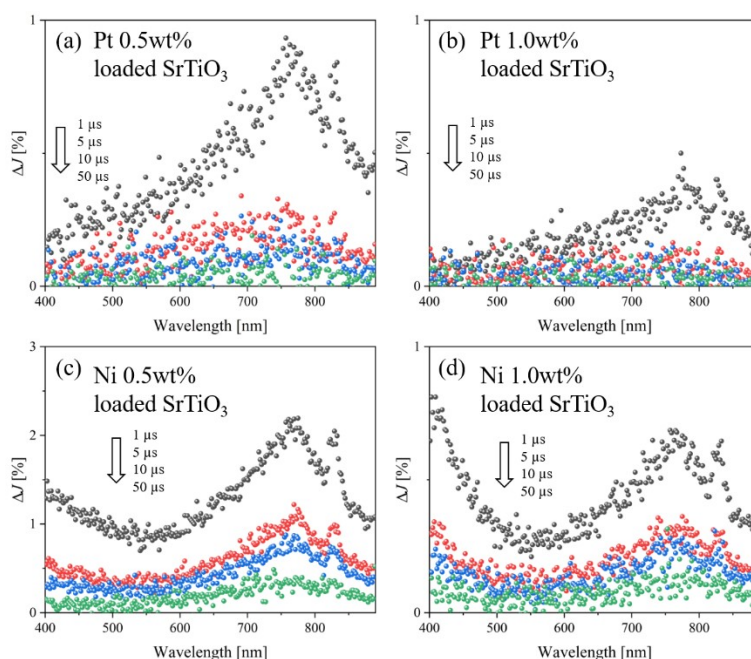**Figure S7. Decay curves of transient absorption of the SrTiO₃ at 825 nm.**

Figure S8. Transient absorption spectra of Pt (a) 0.5wt% and (b) 1.0wt% SrTiO$_3$ particles and Ni (c) 0.5wt% and (d) 1.0wt% SrTiO$_3$ particles irradiated by UV (355 nm) pulsed laser under N$_2$ gas. The pump energy was 1.3 mJ/cm^2, and the repetition rate was 10 Hz.
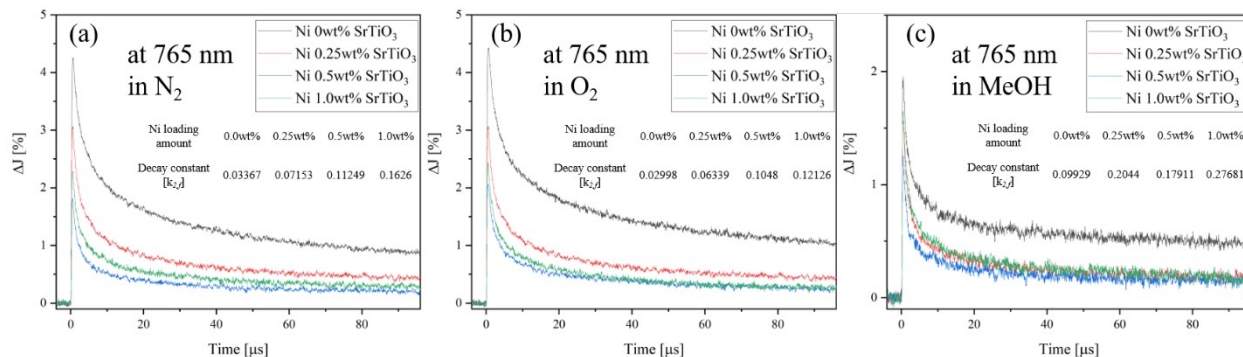

Figure S9. Decay curves of transient absorption of Ni-loaded SrTiO$_3$ in (a) N$_2$ (b) O$_2$ (c) MeOH atmospheres at 765 nm with different loading amount.

References

1. Ichihara, F.; Sieland, F.; Pang, H.; Philo, D.; Duong, A.-T.; Chang, K.; Kako, T.; Bahnemann, D. W.; Ye, J., Photogenerated Charge Carriers Dynamics on La- and/or Cr-Doped SrTiO$_3$ Nanoparticles Studied by Transient Absorption Spectroscopy. *The Journal of Physical Chemistry C* **2020**, *124* (2), 1292-1302.

2. Sieland, F.; Jenny Schneider, J.; Bahnemann, D. W., Fractal Charge Carrier Kinetics in TiO$_2$. *The Journal of Physical Chemistry C* **2017**, *121*(43), 24282-24291.

3. Wang, S.; Hai, X.; Ding, X.; Jin, S.; Xiang, Y.; Wang, P.; Jiang, B.; Ichihara, F.; Oshikiri, M.; Meng, X.; Li, Y.; Matsuda, W.; Ma, J.; Seki, S.; Wang, X.; Huang, H.; Wada, Y.; Chen, H.; Ye, J., Intermolecular cascaded π-conjugation channels for electron delivery powering CO$_2$ photoreduction. *Nature communications* **2020**, *11*(1), 1149.